EFFECT OF THREE-DIMENSIONAL TOPOGRAPHY ON EARTHQUAKE GROUND MOTION

Liao Zhenpeng[I], Yang Baipo[II], Yuan Yifan[III]

SUMMARY

Effect of a simple three-dimensional topography on earthquake ground motion is first reduced to a two-dimensional problem, and the artificial transmitting boundaries are used to simulate the underlying unbounded elastic medium, then the problem is solved by the finite difference method.

The amplification of horizontal or vertical ground motion due to the presence of a hill or depression is theoretically studied separately; a comparison between the theoretical and the observational results is made, and these results are in reasonable agreement.

Finally, a possible generalized application of the method presented in this paper is pointed out.

INTRODUCTION

The effect of topography on earthquake ground motions is usually treated as a two-dimensional problem (1-3), but, in fact, sometimes it is a three-dimensional one. For example, the field inspections have shown (4) that earthquake damage at the top of an isolated hill is much more serious than that in the neighbourhood of the foot of the hill. Obviously, it is not proper to explain this phenomenon by two-dimensional models. Looking for an analytical solution of three-dimensional topography problem, of course, is very troublesome, and the only result (5) as known to the writers was obtained by means of simple acoustic model. A direct numerical analysis seems to be necessary to solve this kind of problems. But great difficulty owing to the limitation of computer storage space arises for such three-dimensional calculation. To cope with this and simplify the analysis, the base boundary is usually assumed as rigid (6), and the seismic motion is then input from this base. In this paper, the rigid base has been replaced by the transmitting boundary for transient wave analysis (7), and the free ground motion is directly input into the interaction system of a topography and elastic half-space. Obviously, such model is rather realistic and simple.

METHOD OF ANALYSIS

The axisymmetrical models are adopted (Fig. 1 a and b) to show the general characteristics of 3-dimensional topography effect. The hill is of a truncated conical shape, and is welded on the surface of elastic half-space. The topographic depression can be taken as a basin, and its surface is an inverted truncated cone. The medium of these models is assumed to be homogeneous, isotropic and perfectly elastic.

[I] Associate Scientist, [II],[III] Research Associate, Institute of Engineering Mechanics (IEM), Chinese Academy of Sciences.

Let's start with the solution for the effect of a hill on horizontal ground motion. Let $\overline{u}_f$ denote the displacement vector of free field, and $\overline{u}_f|_{z=H}$ denote the displacement on the free ground surface, where H denotes the height of hill. It is assumed that the direction of $\overline{u}_f|_{z=H}$ is along the horizontal x-axis, and its magnitude is a time function $f(t)$. As the hill is bonded on the surface of the half-space, the total displacement in the half-space ($z \geq H$, Fig. 1,a) may be expressed as $\overline{u}_f + \overline{u}^{(1)}$, where $\overline{u}^{(1)}$ denotes the displacement of the scattering waves caused by the hill. And the total displacement in the hill ($0 \leq z \leq H$, $0 \leq r \leq R-H+z$, Fig. 1, a) is denotes by $\overline{u}^{(2)}$. So the solution of the problem turns to be the calculation of $\overline{u}^{(1)}$ and $\overline{u}^{(2)}$, assuming that the input function $f(t)$ is given.

Although the topography models are axisymmetrical, but the ground motion input $\overline{u}_f|_{z=H}$ is non-axisymmetrical, hence, the unknown displacements $\overline{u}^{(1)}$ and $\overline{u}^{(2)}$ must depend on the three cylindrical coordinates r, z and φ. However, from the system of elastic equations, it can be proved that such a three-dimensional problem can be reduced into a two-dimensional one (8), and the cylindrical coordinate components of $\overline{u}^{(i)}$ may be expressed as

$$u_r^{(i)} = A^{(i)} \cos\varphi, \quad u_\varphi^{(i)} = D^{(i)} \sin\varphi, \quad u_z^{(i)} = E^{(i)} \cos\varphi \qquad (i = 1 \text{ or } 2) \tag{1}$$

where $A^{(i)}$, $D^{(i)}$ and $E^{(i)}$ are functions of the two coordinates r and z, and they satisfy the following system of partial differential equations

$$\frac{\partial^2}{\partial t^2}\begin{bmatrix} A^{(i)} \\ D^{(i)} \\ E^{(i)} \end{bmatrix} = [K]\begin{bmatrix} A^{(i)} \\ D^{(i)} \\ E^{(i)} \end{bmatrix} \tag{2}$$

where the differential operator matrix $[K]$ is

$$[K] = \begin{bmatrix} \alpha^2\left(\frac{\partial^2}{\partial r^2} + \frac{1}{r}\frac{\partial}{\partial r} - \frac{1}{r^2}\right) - \beta^2\left(\frac{1}{r^2} - \frac{\partial^2}{\partial z^2}\right), & \alpha^2\left(\frac{1}{r}\frac{\partial}{\partial r} - \frac{1}{r^2}\right) - \beta^2\left(\frac{1}{r^2} + \frac{1}{r}\frac{\partial}{\partial r}\right), & (\alpha^2-\beta^2)\frac{\partial^2}{\partial r \partial z}, \\ -\alpha^2\left(\frac{1}{r}\frac{\partial}{\partial r} + \frac{1}{r^2}\right) + \beta^2\left(\frac{1}{r}\frac{\partial}{\partial r} - \frac{1}{r^2}\right), & -\alpha^2\frac{1}{r^2} + \beta^2\left(\frac{\partial^2}{\partial z^2} + \frac{\partial^2}{\partial r^2} + \frac{1}{r}\frac{\partial}{\partial r} - \frac{1}{r^2}\right), & -(\alpha^2-\beta^2)\frac{1}{r}\frac{\partial}{\partial z}, \\ (\alpha^2-\beta^2)\left(\frac{\partial^2}{\partial r \partial z} + \frac{1}{r}\frac{\partial}{\partial z}\right), & (\alpha^2-\beta^2)\frac{1}{r}\frac{\partial}{\partial z}, & \alpha^2\frac{\partial^2}{\partial z^2} + \beta^2\left(\frac{\partial^2}{\partial r^2} + \frac{1}{r}\frac{\partial}{\partial r} - \frac{1}{r^2}\right), \end{bmatrix} \tag{3}$$

where α and β denote the longitudinal and shear wave velocities of the medium respectively.

The conditions of continuity of displacement and stress at the base of the hill ($z=H$ and $r \leq R$) are given as follows

$$A^{(2)} = A^{(1)} + f(t) \qquad D^{(2)} = D^{(1)} - f(t) \qquad E^{(2)} = E^{(1)}$$
$$\sigma_{rz}^{(1)} = \sigma_{rz}^{(2)} \qquad \sigma_{\varphi z}^{(1)} = \sigma_{\varphi z}^{(2)} \qquad \sigma_{zz}^{(1)} = \sigma_{zz}^{(2)} \tag{4}$$

where

$$\sigma_{rz}^{(i)} = \frac{\partial A^{(i)}}{\partial z} + \frac{\partial E^{(i)}}{\partial r} \qquad \sigma_{\varphi z}^{(i)} = \frac{\partial D^{(i)}}{\partial z} - \frac{E^{(i)}}{r} \qquad (i = 1 \text{ or } 2)$$
$$\sigma_{zz}^{(i)} = \frac{\lambda}{\mu}\left(\frac{\partial}{\partial r} + \frac{1}{r}\right) A^{(i)} + \frac{\lambda}{\mu}\frac{D^{(i)}}{r} + \left(\frac{\lambda}{\mu} + 2\right)\frac{\partial}{\partial z} E^{(i)} \tag{5}$$

One of the special features of our method is that by the continuity of the displacements (the first formula of Eq. 4), the free ground motion is introduced into the system of interaction between the hill and the half-space.

The other boundary conditions at the top and the lateral surface of a hill as well as the horizontal ground surface ($z=H$ and $r>R$) may be derived by means of relevant curve coordinates. According to all these boundary conditions, the two-dimensional functions $A^{(i)}$, $D^{(i)}$ and $E^{(i)}$ can be calculated from Eq. 2. The explicit difference formulas are first derived from Eq.2, then the fictitious points (Fig. 2) are introduced, and the formulas to calculate $A^{(i)}$, $D^{(i)}$ and $E^{(i)}$ at these points can be derived from the relevant boundary conditions. Therefore, if the initial values of $A^{(i)}$, $D^{(i)}$ and $E^{(i)}$ at two consecutive levels are given, it is a simple matter to compute them at any time by a forward time-marching process.

Because of the limitation of computer storage, the artificial boundaries have to be introduced (Fig. 3) to perform the above calculations. It is natural to attempt to introduce an artificial boundary which allows waves to travel through it without reflection. Such boundaries have been provided by reference (7), therefore, the transmitting conditions are so derived that the scattering P or S waves may travel through the base boundary, and Rayleigh surface wave and shear wave may travel through the lateral boundary (8). According to these formulas, $A^{(1)}$, $E^{(1)}$ and $D^{(1)}$ on these artificial boundaries at the instant to come may be calculated from those at the present instant.

To study the effect of topographic depression on the horizontal ground motion, $\bar{u}^{(1)}$ alone should be left and considered as displacement caused by the loads which are applied on the surface of the depression and are equal to the negative values of the stresses caused in the free field. The calculation details are similar to those in dealing with the problem of a hill mentioned above. The effect of a hill or depression on the vertical ground motion can also be analysed in a similar and simpler manner. All formulas for all the above cases can be found in reference (8).

NUMERICAL RESULTS

To obtain necessary information in a relatively broad bandwidth, the input function $f(t)$ is assumed to be an approximate impulse with a duration $T(9)$. All variables are expressed in dimensionless form. Furthermore, it is assumed that the Poisson's ratio is equal to ¼ and the slope angle $\theta = 45°$ (Fig. 1), then these topographic problems are controlled by two parameters: H/R and $\eta = \beta T/R$, where H denotes the height of the hill or the depth of the depression, R, the radius of the base of hill or that of the top of depression (Fig. 1). The parameter H/R describes approximately the shape of the topography, and the parameter η controls the input effective frequency bandwidth and the difference mesh size. The numerical results obtained include the treoretical seismograms on the surface of a hill or depression and its surrounding ground surface for input horizontal or vertical ground motion respectively and the spectral ratios which are equal to the Fourier amplitude spectra of the theoretical seismograms divided by that of the free ground motion (8). Results of one of the four cases are only shown in Fig. 4 and Fig. 5.

DISCUSSION

Effect of an isolated hill on ground motion The amplification of ground motion at the top of a hill is caused by two possible factors, i.e. the vibration of the hill as a whole and the convergence of wave energy propagating from the base of the hill upward. It has been shown from the above computation that if $\lambda \geq R$, where $\lambda = 2\pi\beta/\omega$ denotes shear wavelength with angular frequency ω, the amplification is mainly due to the first factor if the input ground motion is horizontal or due to the second factor if the input ground motion is vertical. The first conclusion can be draw from Fig. 4 and Fig. 5. Fig. 4 shows that the motions at different points of the upper part of the hill are similar to the damped harmonic vibrations with almost the same phase and period. So after the main seismic impulse has passed through, the hill vibrates as a whole in a rocking mode. And it is interesting to note that the spectral ratio reaches the maximum value just at this rocking period. So it may be termed as the predominent period T_0 of the hill. Furthermore it can be seen from Fig.5 that

$$T_0 = 3.2\, R/\beta \qquad (6)$$

for $H/R = 1/3 \sim 2/3$. The formula (6) may be used to estimate the period T_0 for an isolated hill approximately. When the period of free ground surface motion approaches to T_0, that is, shear wavelength $\lambda = 3.2R$, significant amplifications ranged from 100% to 400% will be induced at the top of the hill for $H/R = 1/3 \sim 2/3$. Generally, this amplification will be noticed until $\lambda = 6R$. This estimated amplification is much more larger than that estimated from the 2-dimensional model under an incident SH wave (2). Obviously, as to the explanation of earthquake damage caused by an isolated hill, the 3-dimensional result seems to be more reasonable than the 2-dimensional one.

The amplification of vertical ground motion at the top of a hill is also noticeable, and about 40% to 125% more than the free ground motion.

But it is far less than that due to horizontal ground motion. The explanation of this fact is that the whole vibration of the hill is no longer evident (8), and the amplification is mainly due to the convergence of wave energy propagating from the base of hill upward, so it is comparatively reduced.

Because of the inertia of the hill, the deamplification of ground motion at the foot of a hill is caused by the interaction of the hill and the elastic half-space. The motion over there may be about 50% less than the free ground motion. However, the deamplification is, in fact, restricted within a small range, as $r/R=2$, the spectral ratio approaches to 1. So as the distance from the foot of hill is more than R, effect of the 3-dimensional hill on ground motion can be neglected in practice.

Effect of the topographic depression on ground motion Effect of a 3-dimensional depression on ground motion is far less than that of the hill, the dimension of which is as the same as the former. The maximum amplification, about 20%, takes place at the edge of depression and it is only about a half as much as that of the 2-dimensional case (1). The motion on the bottom of the depression decreases generally, and it is quite different from the results of the acoustic model (5).

Comparison between theory and observation The three-dimensional theoretical results have been compared with the records observed for an isolated hill in an aftershock of the Haicheng earthquake, 1975. To eliminate the effects of seismic source and propagating path on the observational seismograms, the spectral ratio, e.g. the ratio of Fourier amplitude spectra of the motion at the top of the hill to that at the base of the hill, is used, and the peak period of the theoretical spectral ratio has been fitted with observational ones. Based on this fit the R/β of the actual hill can be estimated. The deduced R/β can be compared with that of the actual situation. This comparison has shown that the theoretical deduction and the actual situation are in reasonable agreement (8).

CONCLUSION

The above numerical results and corresponding conclusions are suitable for the case that the shear wavelength λ is not less than the characteristic length of the topograph, R. When $\lambda < R$, the effect of wave motion in the hill must be more significant. To obtain a complete understanding to the effect of 3-dimensional topography on ground motion, it is necessary to consider this case. The method presented in this paper, of course, is quite suitable to study this case.

Aslo this paper provides a new numerical method to study the problem of structure-soil interaction. Instead of the assumption of rigid base on which the seismic motion is input, the transmitting boundaries are used and free ground motion is directly input into the interaction system. So attention should be paid to this method and further investigation should be advanced.

REFERENCES

1. M.D. Trifunac, 1973, "Scattering of the plane SH waves by a semi-

cylindrical canyon", Int. J. Earthq. Engng. Struct. Dyn. 1, 267-281.

2. D. M. Boore, 1973, "The effect of simple topography on seismic waves: Implications for the accelerations recorded at Pacoima Dam, San Fernando Valley, California", Bull. Seism. Soc. Am. 63, 1603-1609.

3. H. L. Wong and P. C. Jennings, 1975, "Effects of canyon topography on strong ground motion", Bull. Seism. Soc. Am. 65, 1239-1257.

4. Ground motion research group of IEM, 1975, "Effects of local topography on earthquake ground motion".

5. S. K. Singh and F. J. Sabina, 1977, "Ground motion amplification by topographic depressions for incident P wave under acoustic approximation", Bull. Seism. Soc. Am. 67, 345-352.

6. R. B. Reimer, R.W. Clough and J.M. Raphal, 1973, "Evaluation of the Pacoima dam accelerogram", PROC, 5th WCEE, Vol. 2, pp. 2328.

7. Liao Zhenpeng, Yang Baipo and Yuan Yifan, 1978, "Feedback effect of low-rise buildings on vertical earthquake ground motion and application of transmitting boundaries for transient wave analysis", IEM, Academia Sinica,Harbin, China.

8. Liao Zhenpeng,Yang Baipo and Yuan Yifan, 1980, "Effect of three-dimensional topography on earthquake ground motion", Earthquake Engineering and Engineering Vibration, 1, 14-33.

9. Z. Alterman and D. Loewenthal, 1972, "Computer generated seismograms", Methods in Computational Physics, Vol. 12, 35-162.

10. D. M. Boor, 1972, "Finite difference methods for seismic wave propagation in heterogeneous materials", Methods in Computational Physics, Vol. 11, 1-36.

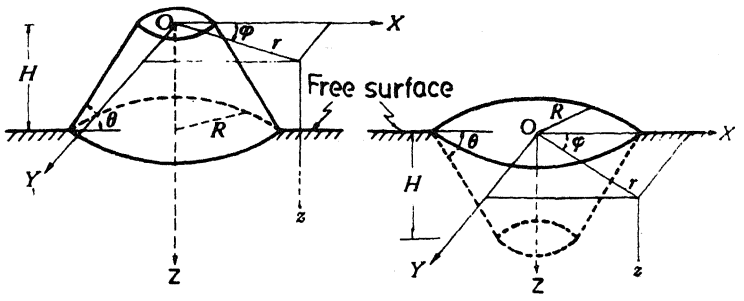

Fig.1. Models of 3-dimensional topography

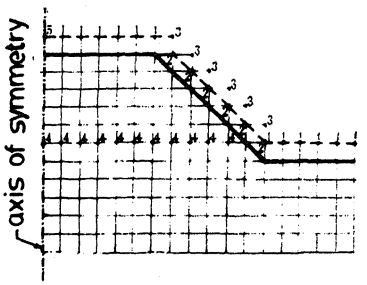

Fig.2. Fictitious points in the hill model

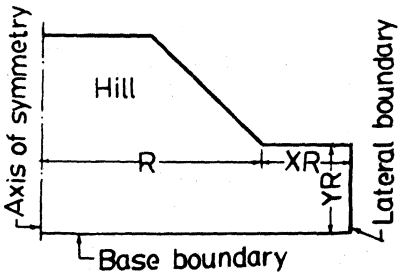

Fig.3. Artificial boundaries

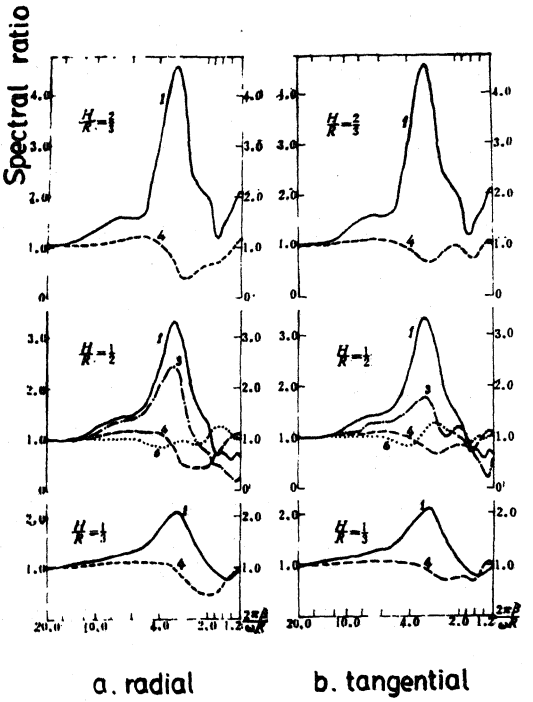

Fig.5. Theoretical spectral ratio (input horizontal motion for the hill)

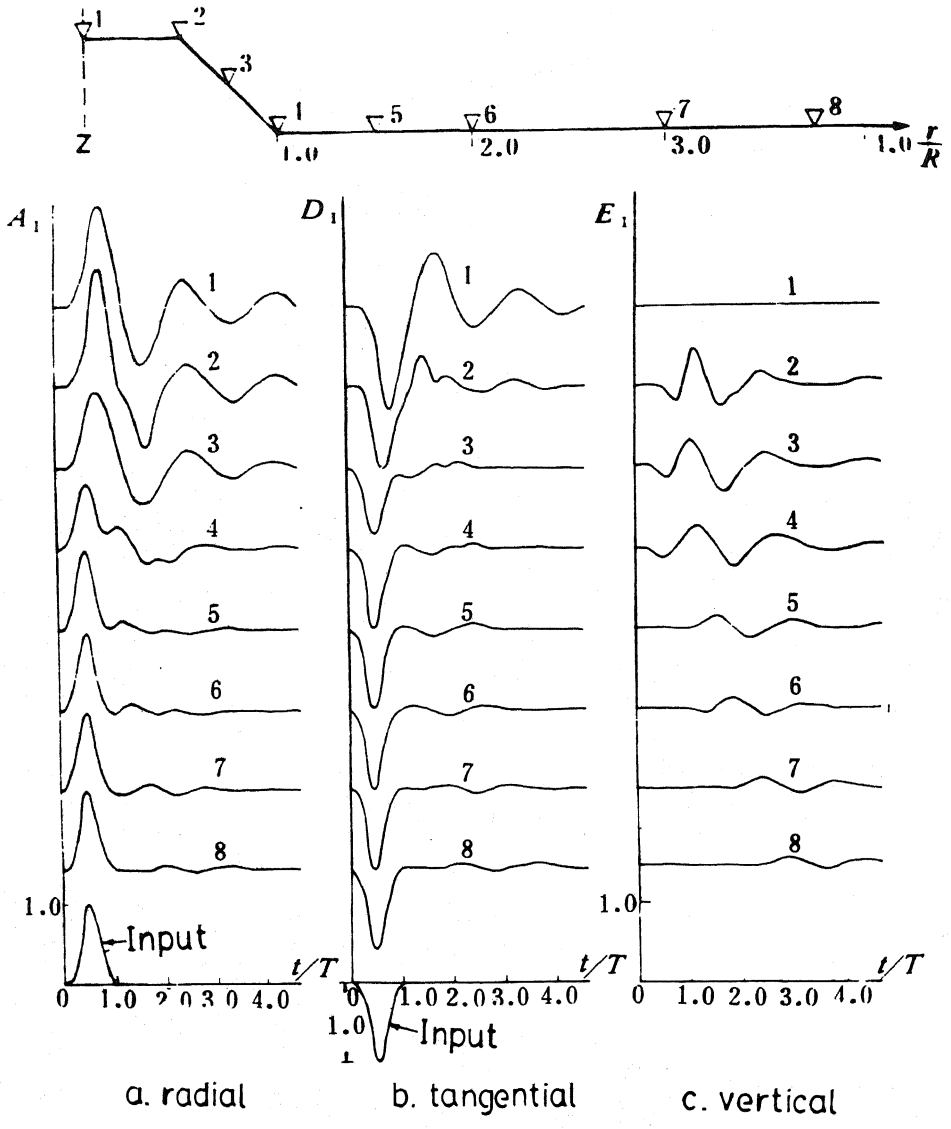

Fig.4. Theoretical seismograms on the hill surface and near by ground surface
(input horizontal ground motion , H/R=1/2)